Global NEST Journal, Vol 26, No 10, 06554

Integrated early flood prediction using sentinel-2 imagery with VANET-MARL-based deep neural RNN

Babu T[1], Raveena Selvanarayanan[2], Tamilvizhi Thanarajan[3] and Surendran Rajendran[4]
[1]Department of Electrical and Electronic Engineering, St. Joseph's College of Engineering, Chennai, 600119, India.
[2]Department of Computer Science and Engineering, Saveetha School of Engineering, Saveetha Institute of Medical and Technical Sciences, Chennai, 602105, India.
[3]Department of Computer Science and Engineering, Panimalar Engineering College, Chennai, 600123, India.
[4]Department of Computer Science and Engineering, Saveetha School of Engineering, Saveetha Institute of Medical and Technical Sciences, Chennai, 602105, India.
Received: 29/07/2024, Accepted: 03/11/2024, Available online: 04/11/2024
*to whom all correspondence should be addressed: e-mail: surendran.phd.it@gmail.com
https://doi.org/10.30955/gnj.06554

Graphical abstract

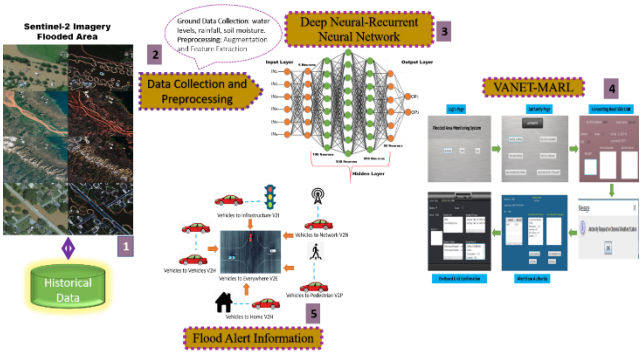

Abstract

Floods are a major contributor to the destruction of infrastructure and the overall economy of afflicted countries, leading to loss of life and significant damage. Remote sensing, satellite imagery photography, global positioning system, and geographic information system (GIS) are commonly used to identify floods and analyze the associated damages. The research presented here integrates Sentinel-2 satellite images, VANET with Multi-Agent Reinforcement Learning (MARL), and a deep neural RNN for early flood prediction. Sentinel-2 imaging delivers extensive geographical and temporal data regarding land cover and water bodies, while VANET-MARL provides real-time ground-truth information and distributed decision-making capabilities. The Deep Neural RNN efficiently acquires intricate patterns from the combined data to forecast the likelihood, intensity, and scope of floods. The experimental findings clearly show that the suggested system outperforms standard methods in terms of accuracy, precision, recall, and lead time. VANET-MARL integration improves the system's ability to adapt and remain strong in changing circumstances. The results showed that the method was 94.8% accurate in early predicting floods.

Keywords: Flood Prediction, VANET-MARL, Deep Neural RNN, Time Series, Sentinel-2 Image, Wireless Vehicle Communication, Weather Report

1. Introduction

The yearly northeast monsoon in November and December 2015 caused excessive rainfall, leading to the 2015 South India floods. The southern Indian states of Andhra Pradesh and Tamil Nadu were hit hard by them, particularly the Coromandel Coast region. The death toll was over 500, and over 1.8 million (18 lakh) people were forced to flee their homes. The floods were one of the most devastating natural disasters of 2015, with damages and losses estimated to be between three and thirteen trillion rupees (US$3 billion) the most expensive calamity to have ever happened in the country Berlin M. A *et al.* (2017). Due to bad climatic conditions, road accidents are tragic, but safety may significantly reduce their impact. Vehicles, motorcycles, bicycles, and pedestrians are all at risk of colliding on the road. Several factors can cause these situations. Vehicle conditions such as bad brakes, tires, or lights may result in a loss of control due to a controlled climate. Road circumstances such as bad weather, poor signage, and uneven surfaces increase the chance of an accident. Road safety is a VANET priority Jizhao.W *et al.* (2024). Vehicles can communicate with each other and roadside infrastructure (V2I) about accidents, risks, and abrupt slowdowns. Real-time data exchange reduces crashes and improves traffic flow. VANETs are benefiting from strong CPUs and 5G connectivity capabilities. This speeds up data transfer, improves network administration, and facilitates ITS integration. Challenges remain despite advances, and obstacles remain. Communication methods must be standardized and secure for widespread usage. Additionally, infrastructure rollout and older car compatibility are ongoing concerns Arun Mozhi Selvi. S *et al.* (2024) On the Rise, VANETs are becoming V2X (Vehicle-to-Everything) communication. V2V (Vehicle-to-Vehicle) cars exchange data like speed, location, and direction,

allowing them to be aware of each other's movements and avoid collisions **Figure 1**. V2I (Vehicle-to-Infrastructure) vehicles communicate with traffic lights, road signs, and sensors to get updates on traffic flow, upcoming hazards, and optimal speed limits. V2P (Vehicle-to-Pedestrian) can improve pedestrian safety by allowing cars to detect people (especially helpful at blind spots) and warn them of potential danger. V2N (Vehicle-to-Network) communication with cellular networks allows for broader data exchange and connection to cloud services. V2N (Vehicle-to-Home) communication is to exchange data directly with a home environment using cellular networks (think LTE,5G) instead of relying on local connections like Wi-Fi. There are other subcategories like V2D (Vehicle-to-Device) for in-car infotainment systems and V2G (Vehicle-to-Grid) for electric vehicles interacting with the power grid. Vehicles can communicate with pedestrians, traffic signals, and even flying cars under these broad-term Techniques Riya Kumarasamy. S *et al.* (2023).

(Vehicular Ad-hoc Network) technology and Deep Neural RNN can further optimize message dissemination and decision-making for drivers which hold immense potential for creating a real-time flood warning system. Vehicles are equipped with On-Board Units (OBUs) that facilitate communication, do data processing, and collect real-time data which act as an RL agent. Roadside Units (RSUs) are strategically positioned in flood-prone locations to gather data, distribute alerts, and transmit information to a central authority Purui. W *et al.* (2020). A central authority oversees the management of real-time data and historical flood data, as well as the distribution of important flood alerts to a broader audience, such as emergency services and navigation applications. Each vehicle (agent) observes its local data and the shared data from neighbors, forming a comprehensive view of the flooding situation in its vicinity. Alotaibi, Y., *et al.* (2024). Deep Learning for the Time Series Forecasting method is utilized to analyze historical water level data and weather patterns to predict future water levels. Surendran, R., *et al.* (2023), this can be particularly useful in capturing complex relationships within the data that traditional machine-learning models. Section 2 provides an examination of the relevant works concerning flood detection strategies, and the rest of the study is structured accordingly. The Proposed VANET-MARL method is detailed in Section 3. Afterwards, in Section 4, we examine the Results and discussion, comparing our performance to that of alternative approaches. The suggested research's key outcomes are finally concluded in Section 5.

2. Related works

Aldweesh A *et al.* (2024) "Mlora-CBF uses simulations to evaluate a novel protocol that uses a modified location routing algorithm in a cluster-based framework. While flooding inside clusters has been used in cluster-based routing, Mlora-CBF addresses resource allocation and network overhead. To evaluate resource allocation and message delivery efficiency, the authors compare their protocol to existing methods using a dataset of mobility patterns, and network density. Chen. X *et al.* (2024), explore a quick and practical VANET IDS using Federated Learning (FL). We examine FL-based IDS for VANETs' algorithms for training local vehicle models and data collection strategies for generating realistic VANET datasets. We contrast centralized versus federated learning methods, emphasizing FL's privacy benefits. Finally, we describe our FL-based IDS for VANETs and its accuracy, efficiency, and privacy benefits. Hemalatha. D *et al.* (2024), novel congestion management technologies that efficiently manage network traffic. This research provides a queue model-based approach to network congestion analysis and a congestion control algorithm. This strategy can optimize data transmission and reduce congestion in MANETs through educated decision-making as illustrated in **Table 1**.

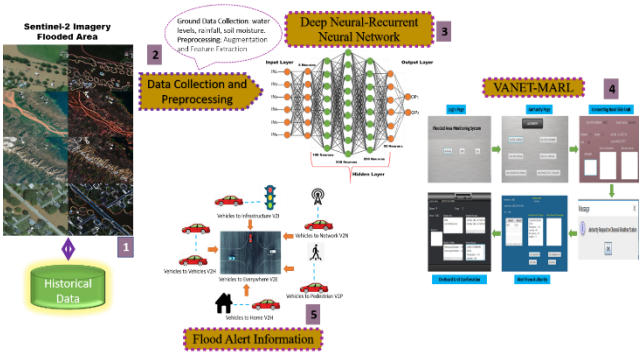

Figure 1. Proposed Model Architecture

3. The proposed model

Research presented VANET-MARL, an automated flood monitoring and alerting emergency strategy. VANET-MARL predicts and classifies flooding, road, accident, water logging, and traffic situations for the public. VANET-MARL involves data standardization, Time series Forecasting-based prediction, and hyper-parameter tweaking. **Figure 2** shows whole VANET-MARL algorithm flow.

3.1. Pattern recognition and feature extraction

Envision yourself operating a vehicle amidst torrential rainfall. Unexpectedly, your car receives a notification indicating a possibility of flooding along the upcoming path. This alert, utilizing VANETs (Vehicular Ad-hoc Networks) with pattern recognition and feature extraction, has the potential to prevent loss of life. Real-time data like rainfall intensity and duration are fed from nearby weather stations. VANET vehicles such as cars, buses, and bikes act as mobile sensors **Figure 2**. GPS Location identifies areas with flooded roads. Wiper Sensor detects increased wiper usage, potentially indicating heavy rain. Image/Video from Dash-cams can capture visual evidence of flooding. Patterns are recognized using sudden spikes in rainfall intensity this could indicate a downpour that might overwhelm drainage systems correlation between high rainfall and previous flood events in the area. Changes in traffic flow patterns sharp drops in speed or unusual congestion could signal road closures due to flooding. From the raw data and recognized patterns, the system extracts critical features for flood detection. The rate of change of rainfall has a rapid increase suggesting a higher flood risk. Combined analysis of rainfall data and GPS location

identifying areas with both heavy rain and reports of flooded roads. Analysis of dash-cam footage to identify water levels or submerged roads.

Table 1. Provides the Overall Flood Detection Comparison of Exisiting Model

Author & Reference	Overview of Existing Approach		
	Algorithm	**Methodology**	**Achieved**
M. Adil *et al.*	Reinforcement Learning (RL) with ANN	Agent-based environment, reward function, training, evaluation	Real-time detection, high accuracy, low false positive rate
D.Amitrano *et al.*	Support Vector Machine, Random Forest, Deep Learning	Feature extraction, classification, change detection	High accuracy, precision, recall)
P. Zhong *et al.*	YOLOv4	Image preprocessing, data augmentation, transfer learning	89.29% mAP for water depth recognition
P.K Jangid *et al.*	Hybrid (CNN+RNN)	Combined strengths, spatiotemporal analysis, flood evolution modeling	Early flood warning, flood impact assessment
H. Farhadi *et al.*	Multi-Layer Perceptron	Preprocessing, feature extraction, classification, evaluation using R2	Achieved R2 of 0.91 for estimating lake area.
M. Mishra *et al.*	MADD	Decentralized multi-agent RL with communication, considering sensing and localization constraints.	Achieved high coverage with minimal communication overhead.
S. Sean *et al.*	ResNet-34	Deep learning, image classification	Accurate road mapping in remote areas
S. Jialin *et al.*	Segment Anything Model (SAM), Random Forest	Automated sample generation, crop classification	Improved crop mapping accuracy (F1-score 0.97-0.996)
D. Aayush *et al.*	Weakly supervised learning	Encoder-decoder architecture, attention mechanism	Fine-grained textual descriptions from satellite images without labeled data
N. Suneth *et al.*	Geometrical Variation Analysis	Landslides in Different Geological Settings Using Satellite Images	Accurate road mapping in remote areas
R.Prathap Kumar *et al.*	clustering, anomaly detection	Features used, training/testing data	Detection accuracy, false positive rate, computational overhead
F. Waqar *et al.*	Cluster-based	Simulation using SUMO, NS-3	Improved packet delivery ratio by 20% compared to AODV

3.2. Time series forecasting based stationarity of data

The structure of the data used for flood detection consists of time series measurements, where each data point represents a specific observation at a particular time (Past, Present Data). The data could include water level sensor readings to indicate the water level at specific locations on the road network. The timestamp of each data point should have a corresponding timestamp to indicate the time of the observation. Depending on the system's complexity, other sensor data like Rain Gauge, Water level sensors such as ultrasonic and pressure sensors, and soil moisture sensors. Road traffic sensors. Radar can detect precipitation and even differentiate between rain, hail, and snow. rainfall readings or atmospheric pressure measurements might also be included to improve flood prediction accuracy. Time series data can be stationary and non-stationary. Stationary data are daily temperature readings in a particular city that might show fluctuations around an average temperature, with no consistent rise or fall over a long period. Non-stationary data are global average temperatures over several years would likely show an upward trend, indicating non-stationarity. The Augmented Dickey-Fuller (ADF) test EQ 1 and the Kwiatkowski-Phillips-Schmidt-Shin (KPSS) test EQ 2 are two common statistical tests used to assess the stationarity of time series data. Unit root detection by ADF Test indicates non-stationarity.

$$\text{ADF Statistic} = \alpha\left(\text{estimated coefficient of } \text{Wt}-1\right) \quad (1)$$

$$\text{LM Statistic} = \text{LM}\left(\Sigma et^2\right) \quad (2)$$

where α is a numerical value, et are the residuals from the regression and LM represents a specific Lagrange Multiplier function. Data with a unit root exhibits a trend or random walk pattern, making future predictions difficult. ADF tests compare statistics against critical values. Stationarity is concluded if the statistic is less negative than the critical value at a particular significance level, rejecting the unit root null hypothesis. But the KPSS Test does the reverse. The null hypothesis is stationarity, and it seeks trends or seasonality. If the KPSS test statistic is greater than critical, stationarity is rejected and trends are present. Suppose the ADF statistic is highly negative (less than the critical value for rejection) and the KPSS statistic is low (not exceeding the critical value). In that case, it suggests strong evidence for stationarity. Similarly, If the ADF statistic is not significant (fails to reject the null hypothesis) or the KPSS statistic is high (indicating trends), the data is likely non-stationary. Converting Non-Stationary Data into Stationary

Data If the data is found to be non-stationary, it may require preprocessing to transform it into a stationary form using differencing and detrending.

3.3. VANET technology with time series analysis

VANET technology can enhance time series analysis for flood detection by facilitating real-time data collection and dissemination across vehicles. On-board units (OBUs) in Vehicles are equipped with OBUs that have sensors and communication modules that allow vehicles to communicate with each other (V2V) and with roadside units (V2I) if deployed. The processing unit can perform basic data analysis and collaborate with the time series analysis system. vehicles share collected data with neighboring vehicles, pedestrian, and nearby homes within their communication range as shown in Pseudocode 1&2.

$$V_{2Vt} = f_{V2V}(Tt, Vt-1, Vt, Dt) \quad (3)$$

Where EQ 3, Where V_2Vt represents the communication between vehicles at time t, Tt denotes the time series data related to traffic conditions, Vt−1 and Vt represent the states of neighboring vehicles at times t−1and t respectively, and Dt represents the distance between vehicles at time t.

$$V_{2It} = f_{V2I}(Tt, It, Dt) \quad (4)$$

Where EQ 4, V_2It represents the communication between vehicles and infrastructure at time t, Tt denotes the time series data related to traffic conditions, it represents the states of infrastructure (e.g., traffic signals, road sensors) at time t, and Dt represents the distance between vehicles and infrastructure at time t.

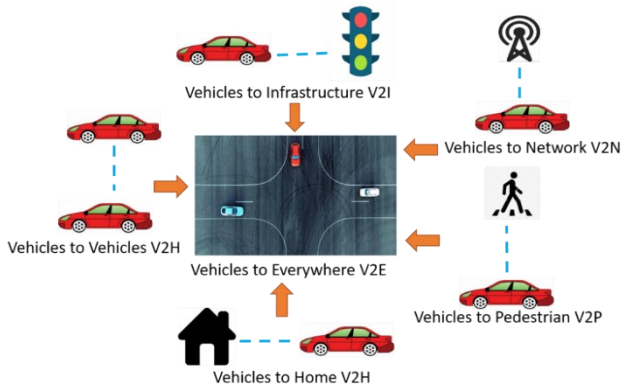

Figure 2. Wireless Vehicle Communication

$$V_{2Pt} = f_{V2P}(Tt, Pt, Dt) \quad (5)$$

Where EQ 5, V_2Pt represents the communication between vehicles and pedestrians at time t, Tt denotes the time series data related to traffic conditions, Pt represents the states of pedestrians (e.g., location, movement patterns) at time t, and Dt represents the distance between vehicles and pedestrians at time t.

$$V_{2Ht} = f_{V2H}(Tt, Ht, Dt) \quad (6)$$

Where EQ 6 V_2Ht represents the communication between vehicles and handheld devices at time t, Tt denotes the time series data related to traffic conditions, Ht represents the states of handheld devices (e.g., smartphones, tablets) at time t, and Dt represents the distance between vehicles and handheld devices at time t.

$$V_{2Nt} = f_{V2N(Tt,Nt)} \quad (7)$$

VANET data encryption comprises sensitive real-time information, including vehicle positions, sensor data, and inter-vehicle communication. Illegal access to this data could threaten the privacy and security of users. The system employs end-to-end encryption (e.g., AES-256) to guarantee that all data sent among cars, roadside units, and the central flood prediction system is secured. This makes it very unattainable for unauthorized third parties to intercept and decipher the data. The exchange of VANET data among cars, roadside units, and the flood prediction system must be secure to prevent man-in-the-middle assaults. The system employs secure communication protocols, including TLS (Transport Layer Security) and IPsec (Internet Protocol Security), for data transmission. This guarantees that data remains encrypted throughout transit, so thwarting any unauthorized interception or alteration.

Pseudocode 1: Vehicle Communication Protocol

function Vehicle_Transmit(message) // Broadcast the message to all vehicles within range

broadcast(message)

end function

function Vehicle_Receive () // Continuously listen for incoming messages

while True:

message = receive () // Process the received message

if message.type == "Traffic Update": // Update the local traffic map

elif message.type == "Hazard Warning": // Display a warning to the driver

end function

Pseudocode 2: Vehicle Communication to Road Side Unit Protocol

function Vehicle_Transmit_to_RSU(message) // Find the nearest RSU

nearest_rsu = find_nearest_rsu() // Send the message to the RSU

send (nearest_rsu, message)

end function

function RSU_Receive() // Continuously listen for incoming messages from vehicles

while True:

message = receive ()// Process the received message based on its type

if message.type == "Traffic Update": // Aggregate traffic data from multiple vehicles, Update a centralized traffic management system

elif message.type == "Vehicle Location": // Update the location of the vehicle on a digital map

end function

3.4. Deep neural-RNN with time series forecasting

Data is collected from vehicles equipped with On-Board Units (OBUs) in a VANET network and historical data are preprocessed and feature extracted for accurate flood detection. The input layer of the neural network with each circle represents a single neuron in the layer **Figure 3**. In flood prediction, these inputs represent factors like past and present rainfall amount, road conditions, climatic conditions, nearby river level, and soil moisture. Single hidden layer with 100 circles. Each circle represents a neuron in the hidden layer. Each connection has an associated weight, which determines the strength of the signal transmitted between neurons.

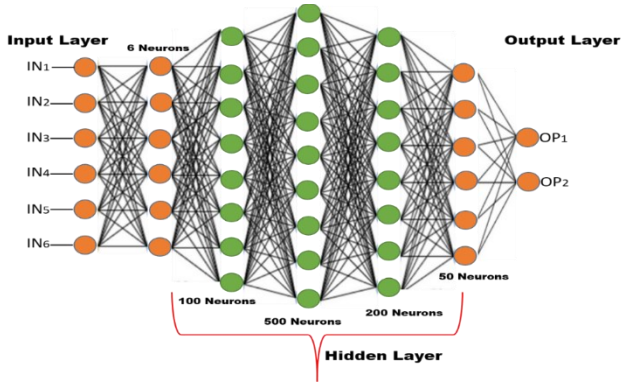

Figure 3. Deep Neural-Recurrent Neural Network

The neural network learns these weights during the training process. The neurons process the signals received from the input layer and apply an activation function to determine the output they send to the next layer. The number of neurons in the output layer depends on the hidden network. In a binary classification task, there would be one neuron for each class (e.g., flood / no flood). With two output neurons, the network may be predicting a binary outcome or two separate values.The model is initialized with the parameters of weights and biases using pre-trained weights. Feed the training data into the network and use backpropagation with an optimization algorithm Adam to adjust the parameters iteratively. Monitor the loss function on the training set and the validation set to ensure the model is learning effectively. Continue training until convergence or until a predefined stopping criterion is met reaching a maximum number of epochs or observing no improvement on the validation set.

3.5. Sentinel – 2 Carries the Multi-Spectral Imager (MSI) of Flooding

Earth Observation Platform to access Sentinel-2 data through Earth Observation Platforms which is an online portal that allows you to search for, download with 13 different bands, covering visible, near-infrared, and short-wave infrared ranges. Explore Sentinel-2 imagery of floods on roads Sentinel-2 data is typically downloaded in TIFF (Tagged Image File Format) format **Figure 4**.

preprocessing the satellite imagery using radiometric and geometric correction, cloud detection and removal and image normalization. feature extraction from Sentinel-2 imagery using normalized difference water index, temporal analysis, and integration into the deep neural RNN Model.

Figure 4. Sentinel-2 Captured Flooded Image

4. Implementation and Results

The research initiative emphasizes on utilizing satellite imagery to identify floods and subsequently transferring this data to automobiles through a VANET for prompt cognizance.

4.1. Collection of dataset discussion

The analysis incorporates Python 3.8, the Keras library, and various additional technologies. The tests were conducted on an Intel i5 processor running at a clock speed of 2.20GHz, 12 GB of RAM, and a dedicated graphics card with a capacity of 2 GB. The Sentinel-2 captured flooded images trained by utilizing the Keras framework. The application programming interface is widely recognized and can function in conjunction with Tensor Flow. The collected 620 datasets are divided into 60:20:20 ratios for training, validation, and Testing.

4.2. Performance Evaluation Compared with Deep Neural RNN

Accuracy is the proportion of correct flood predictions to total predictions eq 8. Precision is the proportion of true positive predictions to all positive predictions eq 9. Recall (Sensitivity) is the proportion of true positive predictions to all actual positive cases eq 10. F1-score is the harmonic mean of precision and recall eq 11. False Positive Rate (FPR) is the proportion of false positive predictions to all negative cases Eq 12. False Negative Rate (FNR) is the proportion of false negative predictions to all positive cases Eq 13. Mean Absolute Error (MAE) average absolute difference between predicted and actual flood levels Eq 14. Root Mean Square Error (RMSE) square root of the average squared difference between predicted and actual flood levels Eq 15 (**Table 2**).

$$\text{Accuracy} = \frac{TP+TN}{TP+TN+FP+FN} \tag{8}$$

$$\text{Precision} = \frac{TP}{TP+FP} \tag{9}$$

$$\text{Recall} = \frac{TP}{TP+FN} \tag{10}$$

$$\text{F1}-\text{score} = 2*\frac{\text{Precision}*\text{Recall}}{\text{Precision}+\text{Recall}} \tag{11}$$

$$\text{FPR} = \frac{FP}{FP+TN} \tag{12}$$

$$FNR = \frac{FN}{TP+FN} \quad (13)$$

$$MAE = \Sigma \quad (14)$$

$$RMSE = \text{sqrt}\left(\Sigma\left(\text{predicted\_level} - \text{actual\_level}\right)\text{^}2 / n\right) \quad (15)$$

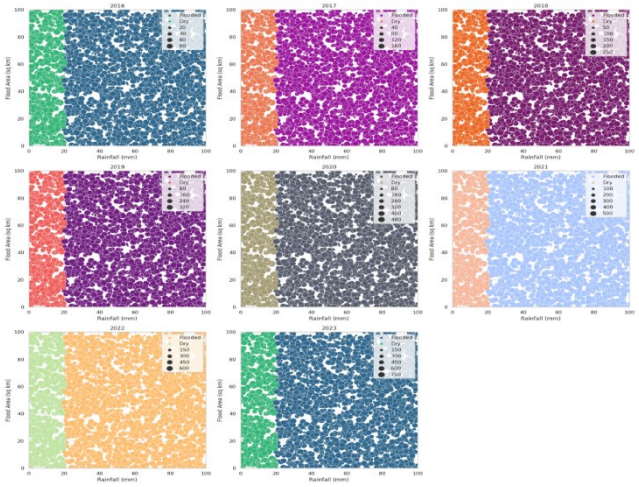

Figure 5. Last 8 Years Flooded Area and Rainfall Observation.

The proposed method achieves 94.8% accuracy, while Convolutional Neural Network, Recurrent Neural Network, Long Short-Term Memory, Generative Adversarial Network, Transformers, and Deep Neural RNN obtain 90.4%, 91.1%, 92.2%, 91.2%, and 92.9%. Existing approaches take longer to calculate all datasets and the suggested technique detects events better than current methods. **Figure 5**, shows the architecture of the flooded area monitoring system. Environmental data is collected from RWI sensors on RSUs. On-board units (OBUs) gather vehicle-related data and location information **Figure 6**. RSUs transfer the gathered data to the governing body. The Data Processing authority analyzes the received data to determine probable flood zones by considering factors such as water level and meteorological conditions. The body disseminating information sends alerts and warnings to On-Board Units (OBUs) to inform drivers of flood conditions. RSUs also provide crucial information to adjacent vehicles. The Feedback Loop with On-Board Units (OBUs) transmits feedback to the governing body regarding road conditions, traffic, and other pertinent data. Authority refers to the primary governing body that is accountable for overseeing the comprehensive administration, analysis of data, and making decisions for the entire system. A Road Side Unit (RSU) refers to a stationary device strategically positioned in certain locations to gather data, establish communication with cars, buses, and bikes, and transmit information to the relevant authority. An onboard unit (OBU) is a device that is mounted in cars to gather real-time data, such as location, speed, and sensor readings, and establish communication with Roadside Units (RSUs). RSUs are equipped with RWI sensors to gather environmental data, such as water level, humidity, and temperature **Figure 7**.

Analyzing Model Performance by analysis of predictions and Ground Truth by conducting a comparison between the filtered flooded regions derived from the Sentinel-2 image (prediction) and the ground truth data, one can evaluate the precision and efficiency of the image processing and segmentation algorithms employed **Figure 8**. Accurate measurement of training, testing, and validation accuracy and loss is essential in the development of flood detection models. Training accuracy quantifies the extent to which the model acquires knowledge from the training data, whereas testing accuracy assesses its effectiveness in handling unfamiliar data. Validation accuracy, however, is utilized to optimize hyperparameters and mitigate overfitting. The training and validation loss measures the model's error during the learning and evaluation processes, respectively. Through the examination of these measures, researchers can evaluate the effectiveness of the model, uncover any problems such as overfitting or under fitting, and make well-informed choices to enhance the flood detection system **Figure 9**.

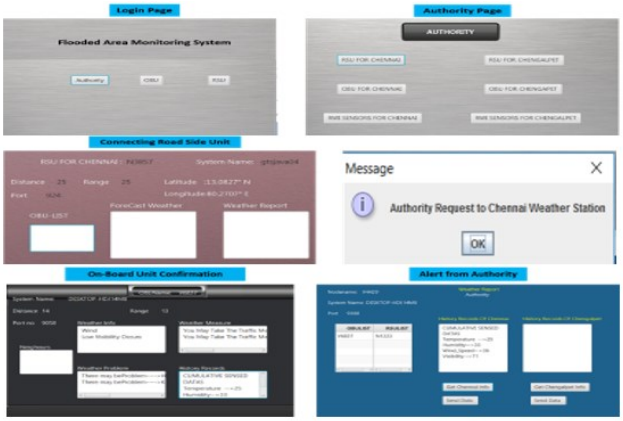

Figure 6. VANET Connectivity using Satellite (Alert Message Generation)

Report ID	Sensor ID	Timestamp	Temperature (°C)	Humidity (%)	Rainfall (mm)	Wind Speed (km/h)	Climatic Condition	Soil Moisture (%)	Road Condition
1	RWI-005	2024-01-01 00:00:00	24.246630	73.671137	1.712870	19.111098	Sunny	36.432762	Flooded
2	RWI-001	2024-01-01 01:00:00	21.076177	54.327203	0.186425	13.237200	Cloudy	51.317692	Flooded
3	RWI-004	2024-01-01 02:00:00	25.682176	75.200501	1.507360	22.922143	Rainy	35.075092	Dry
4	RWI-004	2024-01-01 03:00:00	22.465569	69.847329	1.380423	22.064994	Cloudy	32.732773	Wet
5	RWI-004	2024-01-01 04:00:00	25.964331	51.770697	1.733321	13.684530	Rainy	42.381355	Wet
6	RWI-002	2024-01-01 05:00:00	21.175256	74.329452	0.200184	23.665728	Cloudy	54.315766	Dry
7	RWI-004	2024-01-01 06:00:00	29.758839	68.832671	0.611391	10.602325	Rainy	52.888145	Flooded
8	RWI-003	2024-01-01 07:00:00	29.325612	77.149470	1.308583	21.288597	Cloudy	37.091779	Dry
9	RWI-005	2024-01-01 08:00:00	23.917969	72.461669	0.844036	16.860832	Cloudy	40.000536	Flooded
10	RWI-001	2024-01-01 09:00:00	22.421786	66.833628	1.468151	22.531891	Rainy	59.614428	Wet
11	RWI-001	2024-01-01 10:00:00	22.503982	75.096415	1.715957	16.982290	Cloudy	32.228849	Wet
12	RWI-005	2024-01-01 11:00:00	24.833935	58.341507	0.906608	10.983731	Rainy	32.359441	Dry
13	RWI-003	2024-01-01 12:00:00	20.399928	66.408502	0.868660	13.398183	Cloudy	32.719768	Dry
14	RWI-002	2024-01-01 13:00:00	26.397051	58.808505	0.556938	24.915623	Sunny	39.713268	Dry
15	RWI-001	2024-01-01 14:00:00	24.083029	79.046132	0.010104	15.012664	Rainy	52.915110	Dry
16	RWI-002	2024-01-01 15:00:00	23.774866	56.785889	0.372607	12.484578	Rainy	56.728754	Flooded
17	RWI-002	2024-01-01 16:00:00	28.093650	50.472147	1.959728	22.087462	Cloudy	57.972443	Dry
18	RWI-001	2024-01-01 17:00:00	27.090355	59.775645	1.734572	10.676047	Sunny	37.572208	Flooded
19	RWI-002	2024-01-01 18:00:00	29.543338	65.075282	0.533009	10.996131	Rainy	43.885392	Dry
20	RWI-005	2024-01-01 19:00:00	23.519362	50.850888	1.927498	14.462782	Sunny	32.805239	Flooded
21	RWI-004	2024-01-01 20:00:00	28.975428	66.777449	0.735425	10.711015	Rainy	46.687003	Flooded
22	RWI-001	2024-01-01 21:00:00	27.699672	76.228483	0.595171	24.935690	Cloudy	30.196202	Dry
23	RWI-004	2024-01-01 22:00:00	23.574247	71.141966	0.305615	20.366933	Sunny	43.789009	Dry
24	RWI-001	2024-01-01 23:00:00	26.216654	68.689050	1.803222	17.793797	Sunny	59.412311	Wet
25	RWI-003	2024-01-02 00:00:00	22.885700	78.678853	1.973985	22.077496	Rainy	34.212734	Dry
26	RWI-004	2024-01-02 01:00:00	28.743999	78.748380	0.654823	19.937302	Sunny	36.322690	Dry
27	RWI-001	2024-01-02 02:00:00	21.124273	74.727994	1.406861	12.598974	Cloudy	38.329337	Flooded
28	RWI-002	2024-01-02 03:00:00	22.124344	68.232255	0.670607	13.294587	Sunny	56.003660	Flooded
29	RWI-004	2024-01-02 04:00:00	21.830133	64.632937	0.209981	23.015414	Sunny	56.699794	Dry
30	RWI-004	2024-01-02 05:00:00	24.030260	50.399483	1.785385	15.054420	Cloudy	58.358414	Flooded
31	RWI-004	2024-01-02 06:00:00	27.452330	68.187857	1.103140	16.714605	Sunny	37.452199	Wet
32	RWI-001	2024-01-02 07:00:00	25.269074	79.672642	0.246034	15.867036	Sunny	43.684810	Flooded

Figure 7. Historical Flood Report Dataset collected using RWI Sensor

Figure 8. Sentinel 2 Captured Flooded Area Are Segmented and Compared between Ground Truth and Actual Prediction

Table 2. Performance Analysis Using the Proposed Model

Reference Framework	Approach	(Labeled Data in Training, Validation, and Testing Dataset)					
		Accuracy	Precision	Recall	F1-Score	MAE	RMSE
60% Training Dataset	CNN	92.4%	91.7%	93.1%	92.3%	91.1%	91.3%
	RNN	88.5%	87.1%	89.4%	88.1%	87.1%	88.1%
	LSTM	91.1%	91.4%	92.1%	91.1%	91.1%	91.3%
	GAN	90.1%	89.1%	91.7%	90.3%	90.4%	91.1%
	Transformers	96.7%	95.7%	97.1%	96.7%	94.1%	93.1%
	DN-RNN	94.1%	93.4%	95.1%	94.1%	94.1%	93.3%
20% Validation Dataset	CNN	90.4%	89.1%	91.1%	90.1%	91.1%	92.1%
	RNN	85.9%	84.4%	86.4%	85.6%	84.3%	86.1%
	LSTM	92.4%	93.7%	91.1%	92.4%	92.7%	91.7%
	GAN	88.0%	87.1%	89.1%	88.1%	88.1%	90.4%
	Transformers	91.2%	91.5%	90.5%	90.5%	90.5%	90.1%
	DN-RNN	94.2%	93.5%	95.5%	94.5%	93.5%	95.1%
20% Testing Dataset	CNN	88.3%	87.7%	89.4%	88.7%	88.7%	87.7%
	RNN	83.7%	82.1%	84.1%	83.1%	82.1%	82.3%
	LSTM	90.3%	89.3%	91.5%	90.1%	90.1%	91.1%
	GAN	86.4%	85.5%	87.4%	86.5%	86.5%	87.4%
	Transformers	92.9%	91.7%	93.7%	91.7%	92.7%	91.7%
	DN-RNN	94.8%	92.1%	93.9%	92.3%	93.1%	92.1%

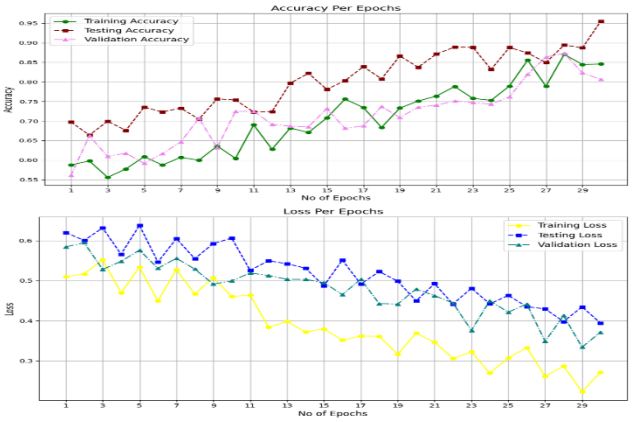

Figure 9. A) Training, Testing, and Validation Accuracy, B) Training, Testing, and Validation Loss

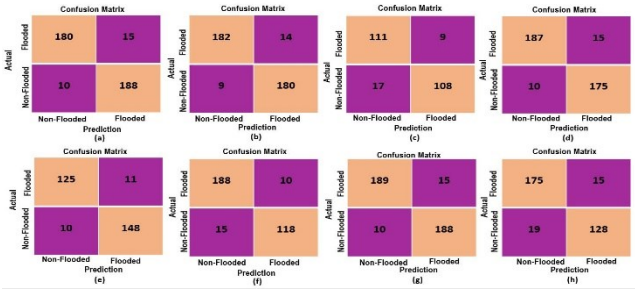

Figure 10. Confusion Matrix of the VANET-MARL Approach

A confusion matrix is a lifeline for assessing the effectiveness of a VANET-MARL strategy in detecting floods. The analysis offers an in-depth examination of accurate and inaccurate forecasts, classifying them as true positives (accurately anticipated floods), true negatives (accurately predicted absence of floods), false positives (incorrectly projected floods), and false negatives (incorrectly predicted absence of floods). Through the examination of the confusion matrix, researchers can evaluate the model's accuracy, precision, recall, and F1-score, providing valuable information about the model's capabilities and limitations in detecting flood situations in the VANET environment **Figure 10**.

4.3. Compared with Other State of Art Methods

Figure 11, presents a comparison between the suggested flood detection system and the most advanced approaches available. Although it does not achieve the highest level of accuracy, the suggested technique effectively identifies flood-affected areas and displays strong performance. Our approach provides complete coverage of various flood scenarios, unlike previous methods that are restricted to specific regions or flood types. The method's distinctive advantage resides in its capacity to identify floods in previously unobserved geographical areas and under varying hydrological circumstances. Its capacity to adjust makes it an adaptable solution for a wide range of flood management concerns. On the other hand, alternative approaches frequently have difficulties in adapting to unfamiliar flood patterns, which restricts their efficacy in practical scenarios.

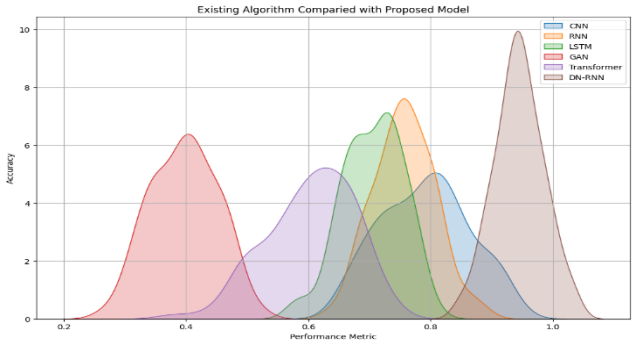

Figure 12. Performance Comparison with Exisiting Model

5. Conclusion

In this research, early flood prediction which is integrated using Sentinel-2 Imagery with VANET-MARL is performed

on real-time datasets incorporated with Deep Neural RNN. Deep neural RNN increases this framework's sequential data analysis and pattern recognition, making flood forecasts more accurate. Local weather stations report rainfall length and severity in real-time. Two prominent statistical tests for stationary time series data are the Augmented Dickey-Fuller (ADF) and Kwiatkowski-Phillips-Schmidt-Shin (KPSS) tests. Autos, pedestrians, and surrounding homes can interact and share data using VANET technology and time series analysis. The integration of Multi-Agent Reinforcement Learning (MARL) with Vehicular Ad Hoc Networks (VANET) results in a flexible system that can adjust to diverse settings and circumstances, offering a resilient solution for a wide range of geographical and climatic situations. The proposed methodology was proven to be effective and efficient by thorough testing on real-world datasets, achieving an accuracy rate of 94.8%. In future research, the model's generalizability depends on adding varied geographical regions and hydrological variables to the dataset. Additional meteorological data like rainfall and humidity can improve prediction accuracy.

6. Ethics Declarations

Funding statement

No funding was received for this study.

Author Contributions

Conceptualization, S.R., and R.S.; methodology, S.R.; software, R.S.; validation, T.T., S.R., and R.S.; formal analysis, B.T.; investigation, S.R.; resources, B.T.; data curation, R.S.; writing original draft preparation, S.R.; writing review and editing, B.T.; visualization, T.T.; supervision, R.S.; project administration, S.R.; funding acquisition, B.T. All authors have read and agreed to the published version of the manuscript.

Conflicts of Interest

The authors declare no conflict of interest.

Experimental statement

No humans, plants, and Animals are disturbed for research work. All image and CSV datasets information regarding water-based processes or applications was obtained from publicly available and ethically sourced data and publications.

Data svailability Statement

raveena, R. (2024). Flood Quality monitoring [Data set]. Zenodo. https://doi.org/10.5281/zenodo.12819030.

Conflict of Interest

The authors declare they have no conflicts of interest to report regarding the present study.

References

Aayush, D., Ahmad, A., Khanal, S., Sastry, S., Kerner, H., and Jacobs, N., (2024). Sat2cap: Mapping fine-grained textual descriptions from satellite images. In Proceedings of the IEEE/CVF Conference on Computer Vision and Pattern Recognition, 1, 533-542.

Adil, M., Midha, S. and Srivastav, V.K., 2024, January. Detection and Prevention of DoS Attack in VANET Using Artificial Neural Network. In 2024 IEEE 1st Karachi Section Humanitarian Technology Conference (KHI-HTC), 1, 1-7.

Aldweesh, A., Kodati, S., Alauthman, M., Aqeel, I., Khormi, I.M., Dhasaratham, M. and Lakshmana Kumar, R. (2024). Mlora-CBF: efficient cluster-based routing protocol against resource allocation using a modified location routing algorithm with cluster-based flooding. Wireless Networks, 30(2), 671-693.

Alotaibi, Y., Rajendran, B. and Rajendran, S., 2024. Dipper throated optimization with deep convolutional neural network-based crop classification for remote sensing image analysis. PeerJ Computer Science, 10, p.e1828.

Amitrano, D., Di Martino, G., Di Simone, A. and Imperatore, P. (2024). Flood Detection with SAR: A Review of Techniques and Datasets. Remote Sens, 16, 656-677.

Arun Mozhi Selvi, S., Alotaibi, Y., Thanarajan, T., and Surendran, R., (2024). Archimedes optimization algorithm quantum dilated convolutional neural network for road extraction in remote sensing images. Heliyon, 10(5), 1-6.

Chen, X., Qiu, W., Chen, L., Ma, Y., and Ma, J. (2024). Fast and practical intrusion detection system based on federated learning for VANET. Computers & Security, 1, 103881-103901.

Farhadi, H., Ebadi, H., Kiani, A. and Asgary, A. (2024). A novel flood/water extraction index (FWEI) for identifying water and flooded areas using sentinel-2 visible and near-infrared spectral bands. Stochastic Environmental Research and Risk Assessment, 14, 1-23.

Hemalatha, D., Cr, K., Ajina, A., Balakrishnan, S., Thangasamy, G., Kuchipudi, R., Dr, P.H.K. And Pallathadka, H. (2024). Novel Congestion Control Mechanism to Improve Performance of Mobile Adhoc Network with Queue Model. Journal of Theoretical and Applied Information Technology, 102(4), 1-29.

Jangid, P.K., Gupta, N., Chandani, P. and Shanmugarathinam, G. (2024). A Novel Neural Network-Based Identification of Flood Regions Using UAV Images. International Journal of Intelligent Systems and Applications in Engineering, 12(3), 369-377.

Jialin, S., Yan, S., Alexandridis, T., Xiaochuang, Y., Zhou, H., Gao, B., Huang, J., Yang, J., and Li,Y., (2024). Enhancing Crop Mapping through Automated Sample Generation Based on Segment Anything Model with Medium-Resolution Satellite Imagery. Remote Sensing, 16(9), 1505.

Jizhao, W., Wu, Z., Liang, Y., Tang, J., and Chen, H., (2024). Perception Methods for Adverse Weather Based on Vehicle Infrastructure Cooperation System: A Review. Sensors, 24(2), 374.

Mishra, M., Poddar, P., Agrawal, R., Chen, J., Tokekar, P. and Sujit, P.B. (2024). Multi-Agent Deep Reinforcement Learning for Persistent Monitoring with Sensing, Communication, and Localization Constraints. IEEE Transactions on Automation Science and Engineering, 1, 1-15.

Prathap Kumar, R., Uppalapati, S., and Reddy Karri, G., (2024). An early detection and prevention of wormhole attack using dynamic threshold value in VANET. International Journal of Vehicle Information and Communication Systems, 9(2), 201-225.

Purui, W., Feng, L., Chen, G., Chenren, X., Wu, Y., Kenuo Xu, X., Shen, G., Du, K., Huang, G., and Xuanzhe, L., (2020). Renovating road signs for infrastructure-to-vehicle networking: A visible light backscatter communication and networking approach. In Proceedings of the 26th Annual International Conference on Mobile Computing and Networking, 2, 1-13.

Raveena. S. and Berlin, M.A. (2017). Broadcasting weather report sto vehicles in urban roads. International Conference on Inventive Systems and Control (ICISC), 1, 1-5.

Riya Kumarasamy, S., Rajendran, S., Andres Tavera Romero, C., and Sendil Murugaraj, S., (2023). Internet of Things Enabled Energy Aware Metaheuristic Clustering for Real-Time Disaster Management. Comput. Syst. Sci. Eng. 45(2), 1561-1576.

Sean, S., Talkhani, R., Huang, T., Engert, J., and William Laurance, F., (2024). Mapping remote roads using artificial intelligence and satellite imagery. Remote Sensing, 16(5), 839.

Suneth, N., Uchida, T., Yamakawa, Y., Hiraoka, M., and Kawakami. A., (2024). Geometrical Variation Analysis of Landslides in Different Geological Settings Using Satellite Images: Case Studies in Japan and Sri Lanka. Remote Sensing, 16(10), 1757.

Surendran, R., Alotaibi, Y. and Subahi, A.F., 2023. Lens-Oppositional Wild Geese Optimization Based Clustering Scheme for Wireless Sensor Networks Assists Real Time Disaster Management. Comput. Syst. Sci. Eng., 46(1), pp.835-851.

Waqar, F., ul Islam, S., Ali Gulzari, U., and Gani, A., (2024). MDVR: a novel multicast routing protocol for unmanned mine detection vehicle (UMDV) communication in VANET. The Journal of Supercomputing, 1, 1-29.

Zhong, P., Liu, Y., Zheng, H., and Zhao, J. (2024). Detection of urban flood inundation from traffic images using deep learning methods. Water Resources Management, 38(1), 287-301.